Available online at www.sciencedirect.com
ScienceDirect
Journal of Molecular Catalysis A: Chemical 285 (2008) 142–149
JOURNAL OF MOLECULAR CATALYSIS A: CHEMICAL
www.elsevier.com/locate/molcata

The effects of synthesis temperature on the structure and visible-light-induced catalytic activity of F–N-codoped and S–N-codoped titania

Yi Xie *, Xiujian Zhao *

Key Laboratory of Silicate Materials Science and Engineering, Wuhan University of Technology, Ministry of Education, Wuhan, Hubei 430070, PR China

Received 8 November 2007; received in revised form 11 January 2008; accepted 15 January 2008
Available online 31 January 2008

Abstract

F–N-codoped and S–N-codoped titania photocatalysts have been synthesized at different temperatures by a chemical procedure. Here titanium tetrachloride, NH_4F and thiourea were used as precursors of titania, fluorine and nitrogen, sulfur and nitrogen, respectively. The as-prepared codoped titania were characterized by X-ray diffraction (XRD), scanning electron microscopy (SEM), transmission electron microscopy (TEM) and UV–visible diffuse reflectance spectra (UV–vis DRS). XRD patterns showed the as-synthesized photocatalysts to be anatase. Increasing reactive temperature from 313 to 413 K enhanced the crystallinity and led to an increase in grain size. UV–vis DRS revealed that the visible absorption ability improved in the range of 400–620 nm with decreasing temperature. Photocatalytic decomposition of methyl orange (MO) carried out in the visible region (≥420 nm) showed that the codoped titania prepared at low temperature possessed over three times of percentage of degradation of MO than that of P25 titania. The mechanism of synthesis of codoped titania at low temperature was also discussed primary.

Keywords: Titania; S–N-codoping; F–N-codoping; Photocatalyst; Low temperature; Visible light

1. Introduction

Non-metal doping has rekindled a great interest in visible-light-induced catalysis in recent years since Asahi et al. [1] first presented the idea of doping titania with nitrogen and other anionic species. Mono-doping of nonmetals including nitrogen [2,3], iodine [4], fluorine [5,6], carbon [7,8] and sulfur [9,10], and codoping of fluorine and nitrogen [11,12], carbon and sulfur [13] have been viewed as effective ways to lower the band gap of titania-based photocatalysts. These technologies consequently enhanced the catalytic activity for degradation of organic compounds under visible or solar light illumination. However, as for the synthesis of nonmetal-doped titania, most experiments were performed at high temperatures, typically from 573 to 873 K.This situation usually results in the increase of the crystallite size and lowering of the surface areas, and thus hampers the enhancement of photocatalytic activity.

On the other hand, large amounts of efforts have been made towards low-temperature preparation of titania photocatalysts. This route is beneficial for the synthesis of titania-based photocatalysts with tuned or controlled morphologies, high surface area and high photocatalytic activity [14]. Tada and co-workers [15] prepared anatase–brookite composite nanocrystals at temperature as low as 323 K by a liquid-phase method. Their composite nanocrystals exhibited high activity for the gas-phase oxidation of CH_3CHO. By using $TiCl_4$ as precursor, titania films were deposited at room temperature and it was found that the amount of rutile in the titania films increased with the annealing temperature lower than 523 K [16]. Weller and co-workers [17] have reported a synthesis of organic-capped anatase titania nanorods by hydrolysis of titanium tetraisopropoxide (TTIP) in oleic acid as surfactant at 353 K. Titania with a diameter of 3 nm and the rutile crystalline phase was synthesized even at room temperature using a water-in-oil microemulsion-mediated system [18]. However, to our knowledge, there were rarely reports

* Corresponding authors. Tel.: +86 27 87652553; fax: +86 27 8766 9729.
E-mail addresses: xieyithanks@163.com (Y. Xie), opluse@whut.edu.cn (X. Zhao).

1381-1169/$ – see front matter © 2008 Elsevier B.V. All rights reserved.
doi:10.1016/j.molcata.2008.01.028

on the systematical synthesis of nonmetal-doped titania at low temperatures.

In our previous work, we had successfully prepared F–N-codoped and S–N-codoped titania photocatalysts that could work efficiently under visible-light irradiation [19,20]. Herein, we further the study of synthesis of the F–N-codoped and S–N-codoped titania photocatalysts, changing the reactive temperatures from 313 to 413 K. The as-synthesized samples were characterized by XRD, SEM, TEM and UV–vis DRS. The experimental results showed that reactive temperature affected not only the spectral absorption of the as-synthesized samples but also the visible-light-induced catalytic degradation for methyl orange (MO) on the F–N-codoped and S–N-codoped titania photocatalysts. We hope that the results in the present paper can extend the research field of low-temperature synthesis of nonmetal-doped titania with strong visible-light response.

2. Experimental

2.1. Photocatalysts synthesis

F–N-codoped and S–N-codoped titania powders were synthesized using the same method as we reported previously [19,20] and the detailed experimental procedure was described in supplementary material (Supplementary material: S1). All chemicals used in the experiments were of analytical grade reagents. A series of F–N-codoped and S–N-codoped titania powders were prepared by changing the reactive temperature: they were designated as FNT-*xxx* and SNT-*xxx*, where "*xxx*" represented the reactive temperature (K). For comparison, commercial Degussa P25 was selected as reference sample.

2.2. Characterization

Powder X-ray diffraction (XRD) patterns were acquired using a D/MAX-IIIA (Rigaku, Japan) diffractometer with Cu Kα radiation at 40 kV, 50 mA in the 20–70° 2θ angle range. Crystallite sizes were calculated from the peak widths using the Scherrer equation:

$$\Phi = k\lambda(\beta \cos\theta)$$

where Φ is the crystallite size, k the shape factor (a value of 0.89 was used in this study), λ the X-ray radiation wavelength (1.5418 Å for Cu Kα), and β is the line width at half-maximum height of the main intensity peak after subtraction of the equipment broadening. Morphologies of the F–N-codoped and S–N-codoped titania particles were examined by a TEM (JEM-2010, Japan) and a SEM. The specimens for TEM were prepared by dropping an ethanol suspension of the powder onto an amorphous carbon foam, supported by a Cu grid. The specimens were allowed to dry under air at room temperature for 20 min. The SEM observations have been carried out with a Hitachi FE S-4800 (Hitachi Ltd., Japan). UV–vis DRS were recorded on Shimadzu UV-2550 UV–Visible Spectrometer (Japan) in the wavelength range of 250–800 nm. $BaSO_4$ was used as the standard for these measurements.

2.3. Photocatalytic activity measurements

The photocatalytic activity of the as-prepared F–N-codoped, S–N-codoped titania and Degussa P25 titania was evaluated by the degradation of MO aqueous solution under visible illumination [19,20]. Here the incident intensity at 420 nm to the sample surface was 190 μW cm^{-2} and the mixtures of photocatalysts and MO solution were magnetically stirred for 30 min in the dark before switching on light. UV–vis spectra of MO were recorded on a UV–vis spectrophotometer (UV-1601, Rigaku, Japan) and the band at 465 nm was used to monitor the effect of the photocatalysis on the degradation of MO. A blank experiment was performed taking MO solution without photocatalyst to know the extent of degradation of MO due to visible radiation.

3. Results and discussion

3.1. Crystal structure

Fig. 1 presents the XRD patterns of the F–N-codoped and S–N-codoped titania synthesized at different reactive tempera-

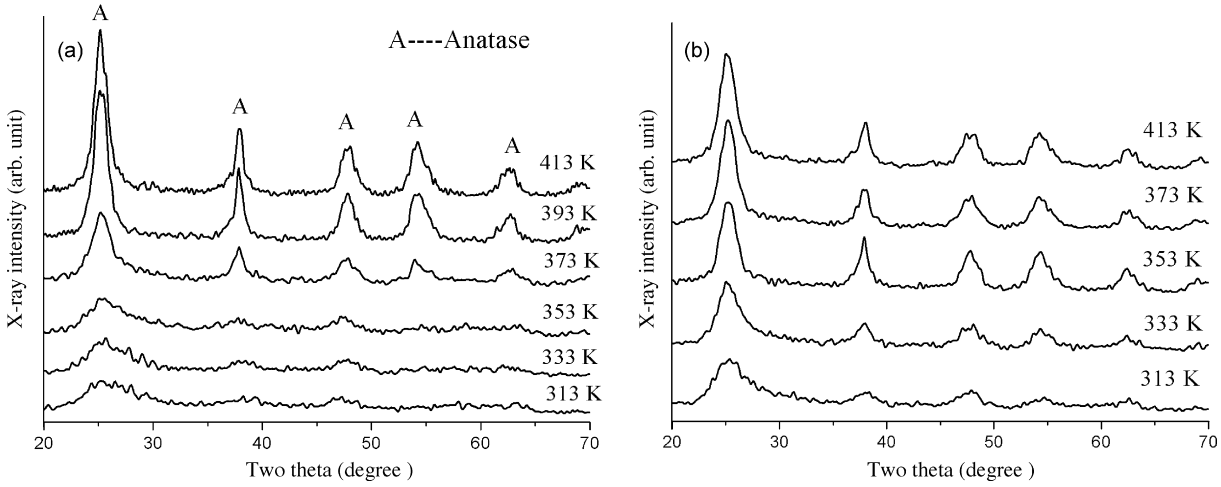

Fig. 1. X-ray diffraction patterns of F–N-codoped (a) and S–N-codoped (b) titania synthesized at different reactive temperatures.

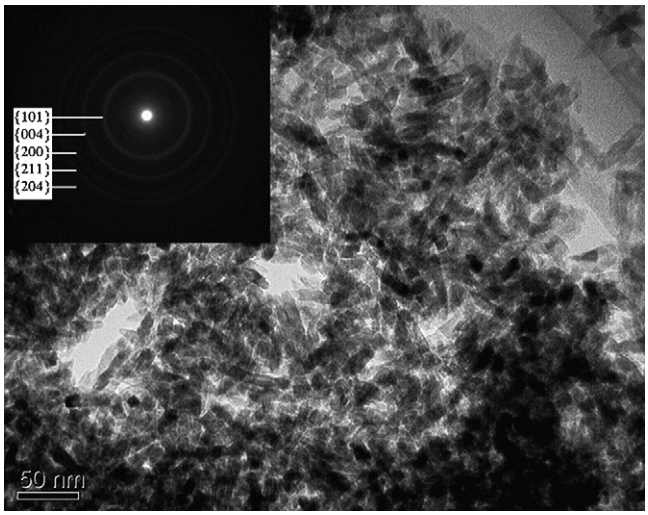

Fig. 2. TEM image of F–N-codoped titania sample as-synthesized at 373 K and corresponding SAED pattern (inset).

tures. The characteristic peaks corresponding to those of titania anatase with different crystal planes (PDF No. 21-1272) were detected for all the samples. The XRD peaks are weak for the samples synthesized at the temperature lower than 353 K, and become stronger with increasing reactive temperature. The weak peaks indicate the poor crystalline structure. On the whole, with the increase of temperature the particles size calculated from XRD data becomes bigger, which is also reflected directly in the XRD patterns with sharper diffraction peaks. For example, the crystallite sizes of samples FNT-373 and FNT-413 are 4.3 and 6.0 nm, and the crystallite sizes of samples SNT-333 and SNT-413 are 3.8 and 5.5 nm, respectively. The XRD patterns shown in Fig. 1 indicate that good crystalline structure could be formed at 373 and 353 K for the F–N-codoped titania and S–N-codoped titania, respectively. Shown in Fig. 2 is the TEM bright field image and selective area diffraction (SAD) pattern (inset) of the sample F–N-codoped titania synthesized at 373 K. Rod-like F–N-codoped titania particles are confirmed also by SAD pattern to be of the anatase crystalline phase.

3.2. UV–vis spectra

Fig. 3 shows the UV–vis DRS of codoped titania synthesized at different reactive temperatures. One of the notable features is that a new absorption band was observed in the visible range of 400–600 nm apart from the fundamental absorption edge of titania. This feature indicates two band transitions for the codoped samples. The first one in the UV region (around 387 nm) is accounted for the titania fundamental band transition. The second in the visible region of 400–620 nm is a resultant of nonmetal codoping. This observation from UV–vis DRS results confirms the presence of two different surface states characteristic of codoped titania. As to the F–N-codoped titania synthesized at temperature lower than 393 K, only a new strong absorption band is observed in the visible range of 400–620 nm. This absorption suggests that the codoped samples can be well activated by visible light. Furthermore, the absorption edge of new band shifts towards higher wavelength on the whole with decreasing reactive temperature for all the codoped titania photocatalysts. For example, the F–N-codoped titania prepared at 313 K shows visible-light absorption up to 620 nm. We observed that the color of the photocatalysts prepared in our experiment became from yellow, light yellow to white with increasing reactive temperature from 313 to 413 K (Supplementary material: S2).

The significant red shift clearly indicates a much decrease in the band gap energy of the as-prepared samples. Fig. 3 (inset) also provides the plots of transformed Kubelka–Munk function versus the band gap energy. The extrapolation of the linear portion of the modified spectra to zero absorption determines the band gap energies of the as-prepared photocatalysts. The band gap energies are estimated as 2.40–3.19 eV and 2.43–3.15 eV for the F–N-codoped and S–N-codoped titania, respectively. Even compared with the optical adsorption of P25 titania (3.0 eV, not shown here), codoped samples in our case showed a strong red shift. In fact, there was F–N-induced midgap for the sample FNT-393, FNT-413 and for all the S–N-codoped titania, which were also roughly estimated to be 2.3–2.4 eV from the inset.

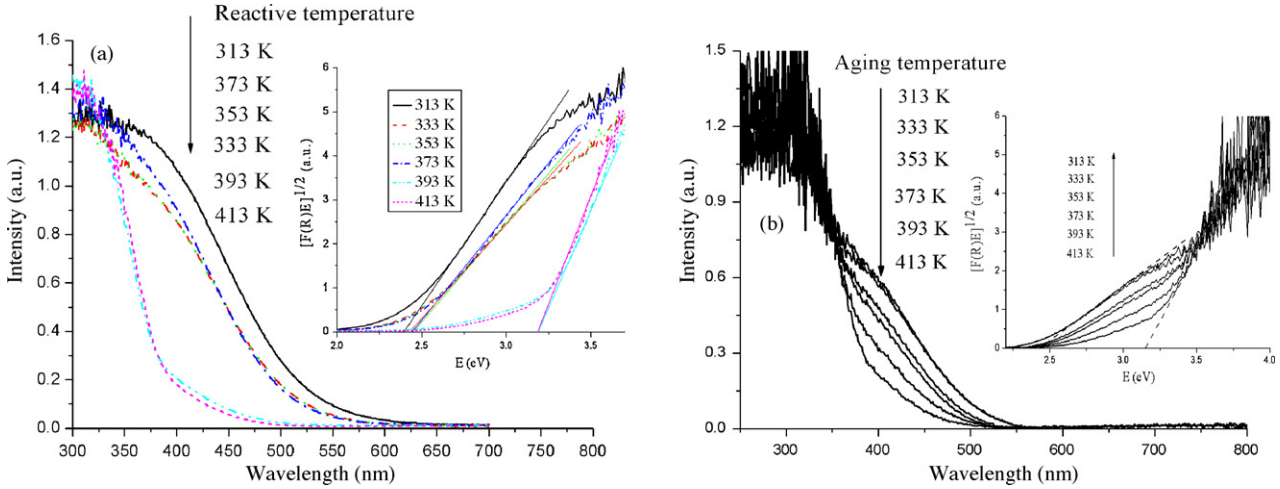

Fig. 3. UV–vis DRS of F–N-codoped (a) and S–N-codoped (b) titania powders. Inset shows plots of the square root of the Kubelka–Munk function ($F(R_\infty)$) vs. the photon energy.

Ohno et al. [9] developed S-doped titania particles, which showed strong absorption for visible light. Using XPS they found that the oxidation state of the S atoms incorporated into the titania particles is S^{6+}. Sulfur was detected as S^{4+} when the molar ratio of thiourea/titania was higher than 1/5 in our previous work [20]. Majima and co-workers [8] prepared S-doped titania using thiourea as S source and they found that the absorption edge was shifted to the lower-energy region due to the S doping that originated from mixing the S 3p states with the valence band (VB). Through band structure calculation, Liu and co-worker [21] viewed anionic S doping as an efficient way to induce visible-light activity for anatase TiO_2 by providing S 3p state on the upper edge of the valence band.

F doping was reported not to affect the optical absorption [11] and cause shift in the fundamental absorption edge of titania [6]. In other case, the spectral absorption of the F-doped titania was found to show a stronger absorption in the UV–vis range and a red shift [5]. The reported calculations for F-doped titania system [22] showed that the F doping gave rise to a modification of the electronic structure around the CB edge of titania, which led to a reduction in the effective bandgap energy and induced the optical responses in the visible-light region.

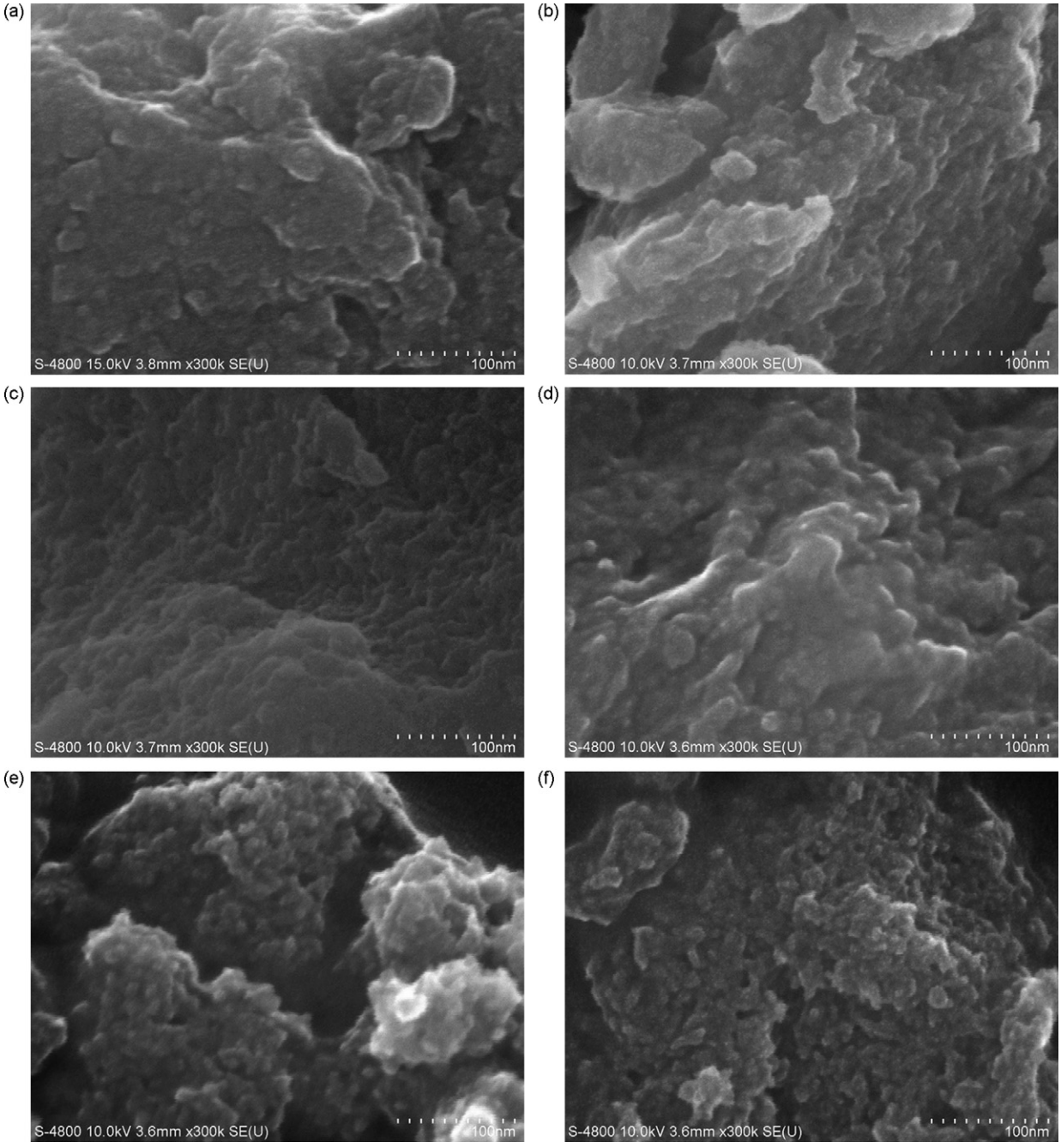

Fig. 4. High magnification FE SEM images of F–N-codoped titania synthesized at different temperatures: (a) 313 K; (b) 333 K; (c) 353 K; (d) 373 K; (e) 393 K; (f) 413 K.

The mechanism of visible-light responses for N-doped titania is also under debate. Asahi et al. [1] attributed the responses for $TiO_{2-x}N_x$ to the band narrowing by mixing of N 2p and O 2p orbitals. Nakato and co-workers [23] reported the mechanism that visible-light responses for N-doped TiO_2 arised from formation of an N-induced (occupied) midgap level slightly above the valence band edge. Sakatani et al. [24] have attributed the visible response to the paramagnetic nitrogen species (such as NO, NO_2, etc.). Nitrogen and fluorine mono-doping has not been compared here because both of them were detected using XPS analysis and nitrogen presented as NO_x species in our recent experiment [19]. Further work for the examination of the mechanism of prominent visible-light response is being under way.

3.3. Morphologies of codoped samples

Figs. 4 and 5 provide the high-magnification SEM images of the F–N- and S–N-codoped titania photocatalysts, respectively. It is obvious that the reactive temperature affects the morphologies of samples. All of the codoped titania powders are found to be rough and agglomerated. Furthermore, the samples prepared

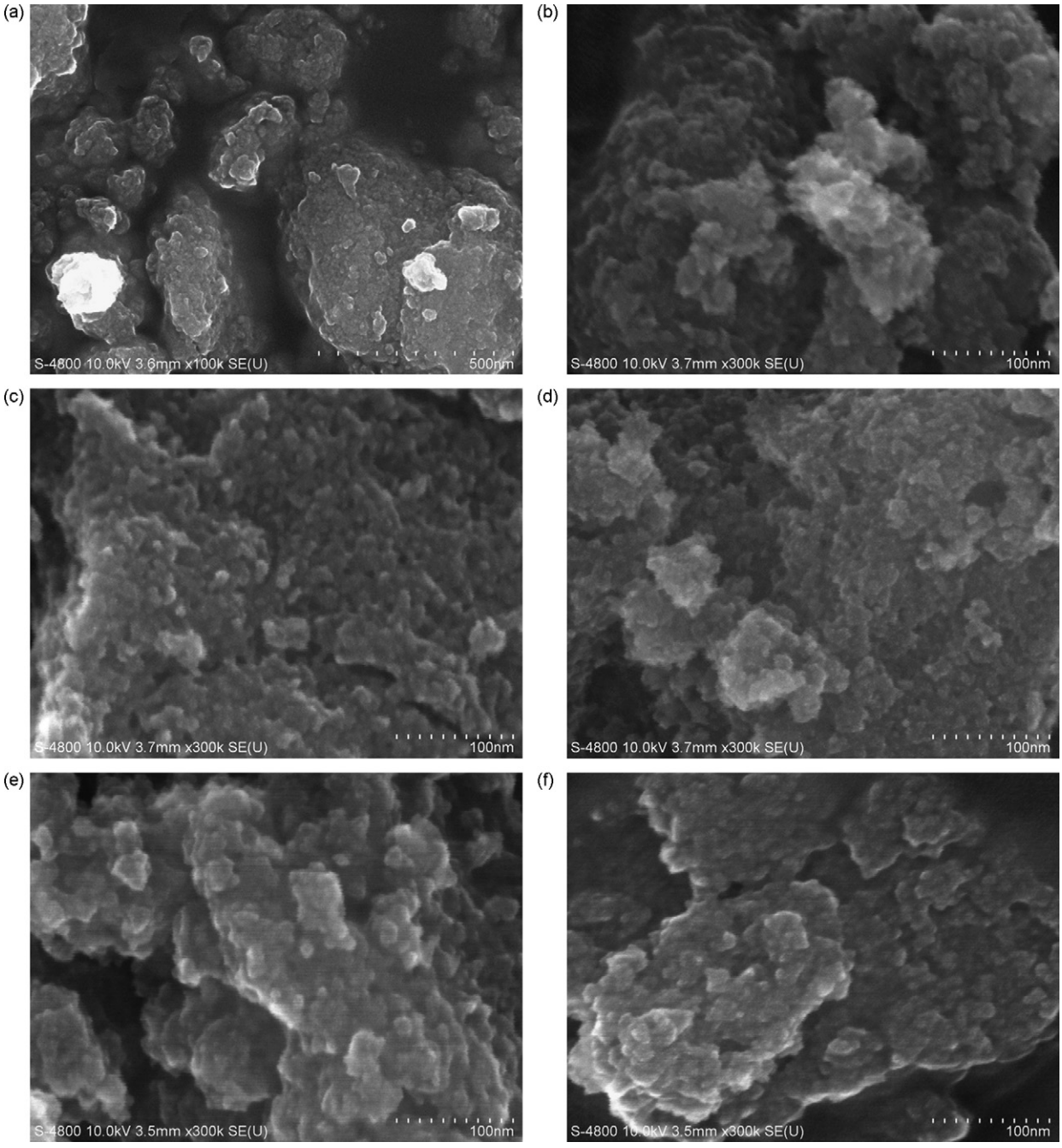

Fig. 5. High magnification FE SEM images of S–N-codoped titania synthesized at different temperatures: (a) 313 K; (b) 333 K; (c) 353 K; (d) 373 K; (e) 393 K; (f) 413 K.

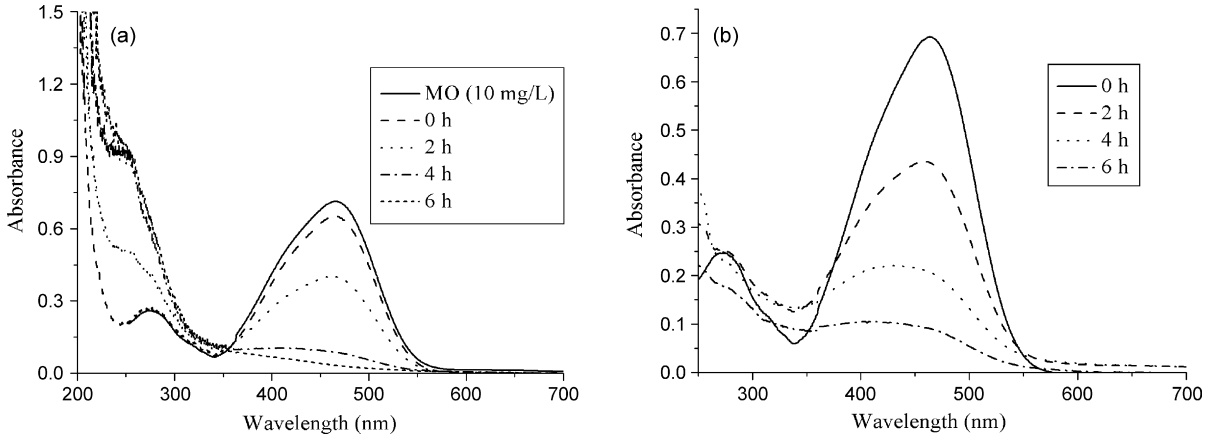

Fig. 6. Absorption spectral changes of MO in the presence of F–N-codoped sample FNT-313 (a) and S–N-codoped sample SNT-313 (b) with different visible illumination time.

at the temperature higher than 353 K display porous structure, which creates void volumes in the photocatalysts. This porous structure becomes more obvious with increasing reactive temperature.

3.4. Photocatalyst activity under visible-light irradiation

To examine the visible-light-induced catalytic property a parallel test was conducted with various as-synthesized codoped titania in MO solution and compared with the activity of a commercial Degussa P25. The blank experiment showed that little bleaching is observed in the absence of the codoped sample even after 12 h of visible radiation (not shown here). However, when MO solution in the presence of F–N- or S–N-codoped titania were illuminated with visible radiation, the absorption band of the visible band at 465 nm decreased with time without a wavelength shift while the band intensity at ~272 nm increased and shifted towards lower wavelength (Fig. 6). After 4 h of irradiation the latter band intensity also started to decrease with time (Fig. 6b). It was reported that the extended aromatic MO absorbs at 465 nm and the aromatic ring absorb in the range 250–272 nm [25]. In the first radiation period the poly aromatic rings in MO started to degrade and created a mono-substituted aromatics, which resulted in the increasing of the band intensity in the range 250–272 nm. With the increasing of irradiation time, the decreasing of this band indicated that CO_2 and H_2O start to form.

A slight decrease in the concentration of MO solution occurred after the powdered samples have been dispersed into the MO aqueous solution for 30 min under no light irradiation (Fig. 7), which was attributed to the adsorption of the titania-based powders for MO molecules. As shown in Fig. 7, the synthesis temperature affected greatly the visible-light-induced catalytic activity. Generally the photocatalytic activity increased initially and decreased with the increasing synthesis temperature. Among them, the samples prepared at the temperature of 313 K showed the highest photodegradation activity among the F–N-codoped and S–N-codoped titania photocatalysts. The photocatalytic degradation rates of sample FNT1 and SNT1 were more than three times higher than that of commercial P25 titania, with a MO conversion of 92.8 and 87.8%, respectively. These results indicate that low-temperature synthesis of nonmetal-codoped titania is an effective way to improve the visible-light-induced photocatalytic activity for decomposition of organic compounds.

Practically, the activity of a photocatalyst for dyes including MO and methylene blue (MB) is affected by many factors such

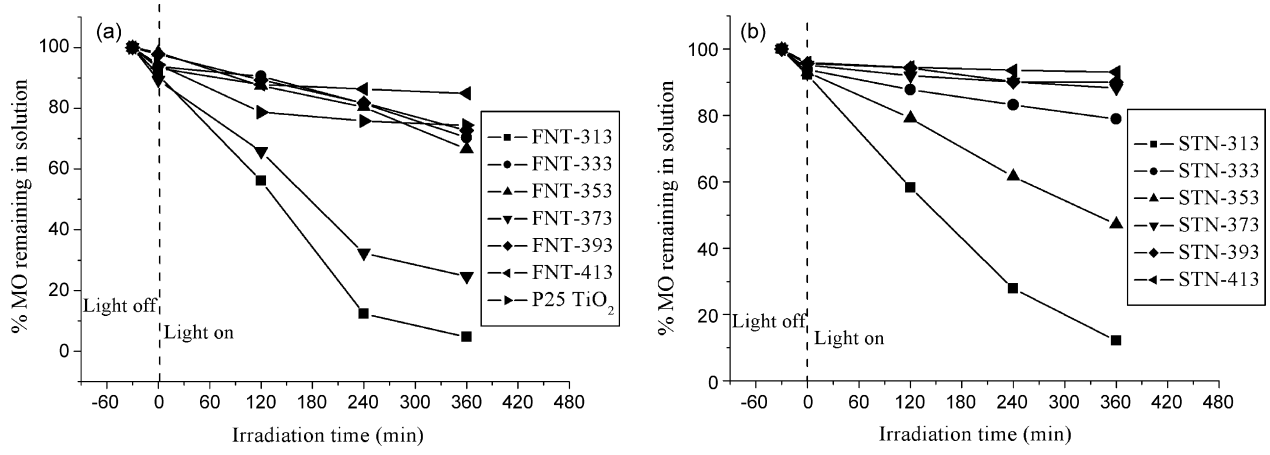

Fig. 7. Visible-light-induced photodegradation of MO in the presence of samples F–N-codoped (a) and S–N-codoped (b) titania. The designated samples FNT-*xxx* and SNT-*xxx* represent the F–N-codoped titania and S–N-codoped titania synthesized at the reactive temperature of *xxx* K.

as surface area, crystallinity, surface hydroxyl density, oxygen vacancies [26], presence of O_2 [27] or H_2O_2 [28], and pH of the solution [29]. Livraghi et al. [30] synthesized N-doped titania via a sol–gel route and they found the activity of N-doped sample in photodegradation of MB was higher than that of bare titania. Using titanium tetrachloride and ammonia as sources, Dai and co-workers [31] prepared N-doped TiO_2 microtubes with high visible-light photocatalytic activity on the degradation of phenol and MO. They attributed this high visible-light-induced catalytic activity to the large specific surface area, surface permeability and well anatase crystallization of N-doped TiO_2. In our case, the reaction solution was not added H_2O_2 and the experiments were processed under the same gaseous and pH conditions. The synthesis temperature affected the crystallinity, grain size and surface area, which consequently resulted in the different recombination rate of electron–hole pair. Furthermore, at wavelengths $\lambda \geq 420$ nm, the intensity of absorption spectra was different for all the samples synthesized at different temperatures. Low-temperature produced samples with strong visible absorbance and red shift towards higher wavelength, which was beneficial to the visible-light-induced decomposition for organic compounds. However, pores structure produced at higher synthesized temperature contributed to the adsorption MO moleculars, which also improved the photocatalytic activity. Overall, the high visible-light-induced catalytic activity of photocatalysts FNT-313, FNT-373, SNT-313 and SNT-353 was attributed to the synergetic effects of strong absorption in the visible-light region, red shift in absorption edge, crystallization, porous structure of the codoped titania photocatalysts.

3.5. Mechanism of low-temperature synthesis of anatase titania

As stated in the first part, low-temperature synthesis of titania-based photocatalysts has attracted much attentions in recent years. Even nanocrystalline rutile titania could be synthesized at low-temperature in the range of 313–423 K [32] and pure rutile nanorods were synthesized by hydrolysis of $TiCl_4$ ethanolic solution in water at 323 K [33]. As to the preparation of titania via sol–gel route using $TiCl_4$ as titanium source, Park and Kim [34] analyzed the occurred reactions in detail. They considered the resulting materials formed by the addition of excess H_2O_2 to the white precipitates as peroxo-titanic acid (PTA) solution. The analysis of FT-IR revealed that this PTA sol was a complicated compound including O–H, Ti–O and O–O bands, which would be transferred to anatase titania after heating from 673 K to 873 K [35]. In our case, codoped titania with good anatase crystallinity was formed even at the temperature of 353 K. We observed that yellow precipitates were formed in a few minutes after addition of thiourea or NH_4F into the PTA solution under stirring. The higher the reactive temperature, the sooner the precipitates formed. Comparatively, the PTA solution was still transparent even after heating at 373 K for 15 h (see Supplementary material: S2).

The phenomena mentioned above indicate that the addition of thiourea or NH_4F improves the production of anatase titania, but the mechanisms of this improvement are different. In a system with thiourea, the deoxidization of the solution leads to the decomposition of the peroxo groups, which consequently improves the crystallization of the PTA. In a system with NH_4F solution, this effect may be attributed to the acidic environment.

4. Conclusions

F–N-codoped and S–N-codoped anatase titania photocatalysts have been synthesized using titanium tetrachloride, NH_4F and thiourea as precursors. Particularly, physical and photocatalytic properties of the codoped photocatalysts prepared at different reactive temperatures have been compared with each other. Increasing reactive temperature from 313 to 413 K enhanced the crystallinity and led to an increase in grain size of the resulting samples from 3.8 to 6.0 nm. F–N- and S–N-codoping resulted in a new strong absorption band in the visible range of 400–620 nm, and with the decreasing reactive temperature the absorption edge shifted toward higher wavelength. Furthermore, the codoped titania synthesized at the temperatures higher than 373 K displayed porous structure and this structure became more obvious with increasing temperature. The high visible-light-induced catalytic activity of F–N- and S–N-codoped titania photocatalysts was attributed to the synergetic effects of strong absorption in the visible-light region, red shift in adsorption edge, crystallization, porous structure of the resulting samples. Overall, the wet chemical process in our work may offer a new method for low-temperature synthesis of nonmetal-doped titania with prominent visible-light-response.

Acknowledgements

This research was financial supported by the Program for Changjiang Scholars and Innovative Research Team in University (PCSIRT, No. IRT0547) and the Cultivation Fund of the Key Scientific and Technical Innovation Project (No. 705036), Ministry of Education.

Appendix A. Supplementary data

Supplementary data associated with this article can be found, in the online version, at doi:10.1016/j.molcata.2008.01.028.

References

[1] R. Asahi, T. Morikawa, T. Ohwaki, A. Aoki, Y. Taga, Science 293 (2001) 269–271.
[2] Y. Wang, C.X. Feng, Z.S. Jin, J.W. Zhang, J.J. Yang, S.L. Zhang, J. Mol. Catal. A: Chem. 260 (2006) 1–3.
[3] A. Ghicov, J.M. Macak, H. Tsuchiya, J. Kunze, V. Haeublein, L. Frey, P. Schmuki, Nano Lett. 6 (2006) 1080–1082.
[4] M.C. Long, W.M. Cai, Z.P. Wang, G.Z. Liu, Chem. Phys. Lett. 420 (2006) 71–76.
[5] J.C. Yu, J.G. Yu, W.K. Ho, Z.T. Jiang, L.T. Zhang, Chem. Mater. 14 (2002) 3808–3816.
[6] D. Li, H. Haneda, N.K. Labhsetwar, S. Hishita, N. Ohashi, Chem. Phys. Lett. 401 (2005) 579–584.
[7] S.U.M. Khan, M. Al-Shahry, W.B.J. Ingler, Science 297 (2002) 2243.
[8] T. Tachikawa, S. Tojo, K. Kawai, M. Endo, M. Fujitsuka, T. Ohno, K. Nishijima, Z. Miyamoto, T. Majima, J. Phys. Chem. B 108 (2004) 19299–19306.

[9] T. Ohno, T. Mitsui, M. Matsumura, Chem. Lett. 32 (2003) 364–365.
[10] S. Yin, K. Ihara, Y. Aita, M. Komatsu, T. Sato, J. Photochem. Photobiol. A: Chem. 179 (2006) 105–114.
[11] D. Li, N. Ohashi, S. Hishita, T. Kolodiazhnyi, H. Haneda, J. Solid State Chem. 178 (2005) 3293–3302.
[12] D.G. Huang, S.J. Liao, J.M. Liu, Z. Dang, L. Petrik, J. Photochem. Photobiol. A: Chem. 184 (2006) 282–288.
[13] H. Sun, Y. Bai, Y. Cheng, W. Jin, N. Xu, Ind. Eng. Chem. Res. 45 (2006) 4971–4976.
[14] D. Wang, F. Caruso, Chem. Mater. 14 (2002) 1909–1913.
[15] T. Ozawa, M. Iwasaki, H. Tada, T. Akita, K. Tanaka, S. Ito, J. Colloids Interface Sci. 281 (2005) 510–513.
[16] K.-J. Kim, K.D. Benkstein, J. Van de Lagemaat, A.J. Frank, Chem. Mater. 14 (2002) 1042–1047.
[17] P.D. Cozzoli, A. Kornowski, H. Weller, J. Am. Chem. Soc. 125 (2003) 14539–14548.
[18] M. Andersson, A. Kiselev, L. Osterlund, A.E.C. Palmqvist, J. Phys. Chem. C 111 (2007) 6789–6797.
[19] Y. Xie, Y.Z. Li, X.J. Zhao, J. Mol. Catal. A: Chem. 277 (2007) 119–126.
[20] Y. Xie, Q.N. Zhao, X.J. Zhao, Y.Z. Li, Catal. Lett. 118 (2007) 231–237.
[21] F.H. Tian, C.B. Liu, J. Phys. Chem. B 110 (2006) 17866–17871.
[22] T. Yamaki, T. Umebayashi, T. Sumita, S. Yamamoto, M. Maekawa, A. Kawasuso, H. Itoh, Nucl. Instrum. Methods Phys. Res. B 306 (2003) 254–258.
[23] R. Nakamura, T. Tanaka, Y. Nakato, J. Phys. Chem. B 108 (2004) 10617–10620.
[24] Y. Sakatani, J. Nunoshige, H. Ando, K. Okusako, H. Koike, T. Takata, J.N. Kondo, M. Hara, K. Domen, Chem. Lett. 32 (2003) 1156–1157.
[25] S. Al-Qaradawi, S.R. Salman, J. Photochem. Photobiol. A: Chem. 148 (2002) 161–168.
[26] M.A. Fox, M.T. Dulay, Chem. Rev. 93 (1993) 341.
[27] A. Mills, J. Wang, J. Photochem. Photobiol. A: Chem. 127 (1999) 123–134.
[28] A.H. Lu, Y. Li, M. Lv, C.Q. Wang, L. Yang, J. Liu, Y.H. Wang, K.-H. Wong, P.-K. Wong, Solar Energy Mater. Solar C 91 (2007) 1849–1855.
[29] K.M. Parida, N. Sahu, N.R. Biswal, B. Naik, A.C. Pradhan, J. Colloids Interface Sci. 318 (2008) 231–237.
[30] S. Livraghi, M.C. Paganini, E. Giamello, A. Selloni, C.D. Valentin, G. Pacchioni, J. Am. Chem. Soc. 128 (2006) 15666–15671.
[31] J.H. Xu, W.L. Dai, J.X. Li, Y. Cao, H.X. Li, H.Y. He, K.N. Fan, Catal. Commun. 9 (2008) 146–152.
[32] M. Nag, P. Basak, S.V. Manorama, Mater. Res. Bull. 42 (2007) 1691–1704.
[33] Y.W. Wang, L.Z. Zhang, K.J. Deng, X.Y. Chen, Z.G. Zou, J. Phys. Chem. C 111 (2007) 2709–2714.
[34] J.-K. Park, H.-K. Kim, Kor. Chem. Soc. 23 (2002) 745–748.
[35] Z.F. Yuan, B. Li, J.L. Zhang, C. Xu, J.J. Ke, J. Sol–Gel Sci. Technol. 39 (2006) 249–253.